Big Bang Nucleosynthesis

Riou NAKAMURA[1], Masa-aki HASHIMOTO[1], Katsuhiko SATO[2,3] and Kenzo ARAI[4]

[1] *Department of Physics, Kyushu University, Fukuoka 812-8581*
[2] *Institute for the Physics and Mathematics of the Universe, The University of Tokyo, Kashiwa, 277-8568*
[3] *School of Science and Engineering, Meisei University, Tokyo 191-8506*
[4] *Department of Physics, Kumamoto University, Kumamoto 860-8555*

(Received September 30, 2010)

Big bang nucleosynthesis is reviewed with taking into account the observed abundance of light elements. We examine the standard big bang nucleosynthesis (SBBN) and confirm that helium abundance is not enough to fix the baryon to photon ratio η. As for deuterium, observational constraint on η agrees well with the value determined from WMAP. It is, however, difficult to reconcile the observations of ^{7}Li with the WMAP constraint. Furthermore, we investigate a simple two-zone model of inhomogeneous big bang nucleosynthesis (IBBN), where we review a series of our recent studies. In a high density region, heavy elements are produced up to the mass number 160. We present several interesting results that may become an important milestone for the origin of the elements in the universe.

§1. Introduction

Primordial nucleosynthesis is one of the best astrophysical sites to understand the origin of the elements,[1)] because it produces the reasonable abundances[2),3)] of light elements, ^{4}He, D and ^{7}Li. The simplest and most trustful theory is called the standard big-bang nucleosynthesis (SBBN), where we assume the cosmological principle that the universe is homogeneous and isotropic in the large scale. Unfortunately, current situation of SBBN cannot be compatible with the observed abundance of ^{7}Li, though observational uncertainties have been pointed out such as the atmospheric model of metal-poor stars[4)] or some unknown physical processes.[5)]

On the other hand, heavy element nucleosynthesis beyond the mass number $A = 8$ has been investigated in a framework of inhomogeneous BBN (IBBN) [6)–11)] The baryon inhomogeneity is induced from baryogenesis[10)] or some phase transitions[11),12)] as the universe cools down during the expansion of the universe. It should be noted that IBBN motivated by QCD phase transition becomes difficult, because the transition has been proved to be crossed over smoothly by the Lattice QCD simulations,[13)] which means that the phase transition occurs between the quark-gluon plasma and hadron phase under the finite temperature and zero chemical potential. Although a large scale inhomogeneity of baryon distribution should be ruled out by cosmic microwave background (CMB) observations,[14),15)] there still be advocated for small scale inhomogeneities within the present accuracy of observations. Therefore, it remains possible for IBBN to occur in some degree during the early era.

The Wilkinson Microwave Anisotropy Probe (WMAP) has derived critical parameters concerning the cosmology of which the baryon to photon ratio η is deter-

mined[15] to be $\eta_{\rm WMAP} = (6.19 \pm 0.15) \times 10^{-10}$. While the uncertainty in the observed abundance of ^{4}He is large, the value $\eta_{\rm WMAP}$ is surely consistent with that obtained from the observation of D. Therefore, we are able to fix $\eta_{\rm WMAP}$ in considering the nucleosynthesis in the early universe. Once η is determined, BBN can be performed along the thermodynamical history with use of the nuclear reaction network (BBN code).[16] On the other hand, peculiar observations of abundances for heavy elements and/or ^{4}He could be understood in the way of IBBN. For example, metallicity of C, N and Si in quasars could be explained from IBBN.[17] Furthermore, from recent observations of globular clusters, possibility of inhomogeneous distribution of He is pointed out,[18] where proposed are some separate groups of different main sequences in blue band of low mass stars due to high primordial helium abundances.[19]

Using recent progress in observations, it could be urgent to re-investigate IBBN as opposed to Ref. 20). It has been found that[21] synthesis of heavy elements for both p- and r-processes is possible if $\eta > 10^{-4}$ and that the high η regions are compatible with the observations of the light elements, ^{4}He and D. However, the analysis is only limited to a parameter of a specific baryon number concentration. Therefore we need to constrain the possible regions in the universe by adopting a two-zone model comparing with available observations.

§2. Thermal evolution of the universe

Based on the cosmological principle or the Robertson-Walker metric, the standard model has been constructed with use of the Einstein equation. In practice, we can follow the evolution of temperature T and energy density ρ by solving the Friedmann equation

$$\left(\frac{\dot{x}}{x}\right)^2 = \frac{8\pi G}{3}\rho, \tag{2.1}$$

where x is the cosmic scale factor and G is the gravitational constant. The total energy density ρ is written as

$$\rho = \rho_\gamma + \rho_\nu + \rho_{e^\pm} + \rho_b,$$

where the subscripts $\gamma, \nu, e^\pm$ and b indicate photons, neutrinos, electrons/positrons and baryons, respectively.

The energy conservation law is given by

$$\frac{d}{dt}(\rho x^3) + p\frac{d}{dt}(x^3) = 0, \tag{2.2}$$

where p is the pressure of the fluid. The equation of state is described as

$$p/\rho = \begin{cases} 1/3 & \text{for photons and neutrinos,} \\ 0 & \text{for baryons.} \end{cases}$$

Therefore, the baryon density varies as $\rho_b \propto x^{-3}$ and the temperature as $T \propto x^{-1}$ except for the era of the significant contribution of $e^\pm$ to the energy density at $T \simeq 5 \times 10^9$ K. We include the effects of $e^\pm$ annihilation on the temperature.[23]

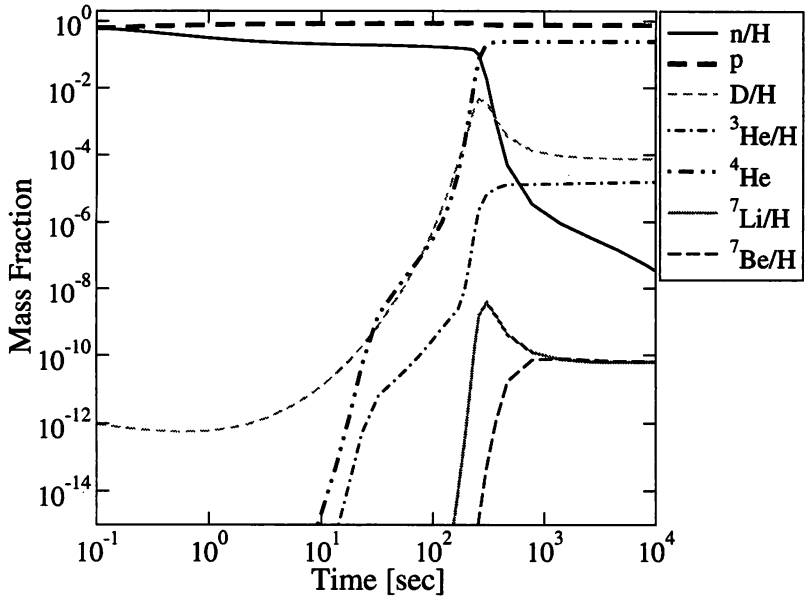

Fig. 1. Evolution of mass fractions in SBBN for $\eta_{\rm WMAP} = 6.19 \times 10^{-10}$.

§3. Standard big bang nucleosynthesis

It has been advocated that SBBN is established to explain the origin of the light elements. We calculate nucleosynthesis with use of the BBN code[16] which contains 24 nuclei from neutron to ^{16}O. We adopt the reaction rates of NACRE,[24] the neutron life time $\tau_N = 885.7$ sec,[25] and take the number of species of massless neutrinos to be $N_\nu = 3$. Figure 1 shows the evolution of main components of light elements for $\eta_{\rm WMAP} = 6.19 \times 10^{-10}$. Significant amounts of D, ^{3}He, ^{4}He, ^{7}Li and ^{7}Be are produced during the first 3 min. However, as has recently been pointed out, there remains a problem in SBBN that is clarified by considering the current observations.

The primordial abundance of ^{4}He, by mass fraction, is[3]

$$Y_{\rm p} = 0.2477 \pm 0.0029, \tag{3.1}$$

which includes the systematic uncertainties in various observations. The number ratio of deuterium is observed[26] to be

$$\mathrm{D/H} = (2.82 \pm 0.12) \times 10^{-5}. \tag{3.2}$$

The observed abundance of ^{7}Li is[27]

$$^7\mathrm{Li/H} = (2.19 \pm 0.28) \times 10^{-10}, \tag{3.3}$$

which is inconsistent with the calculated abundance in SBBN. This problem is difficult to solve at the present stage. In Fig. 2 we show the produced values of ^{4}He, D/H and ^{7}Li/H as a function of η. The line widths for individual elements correspond to

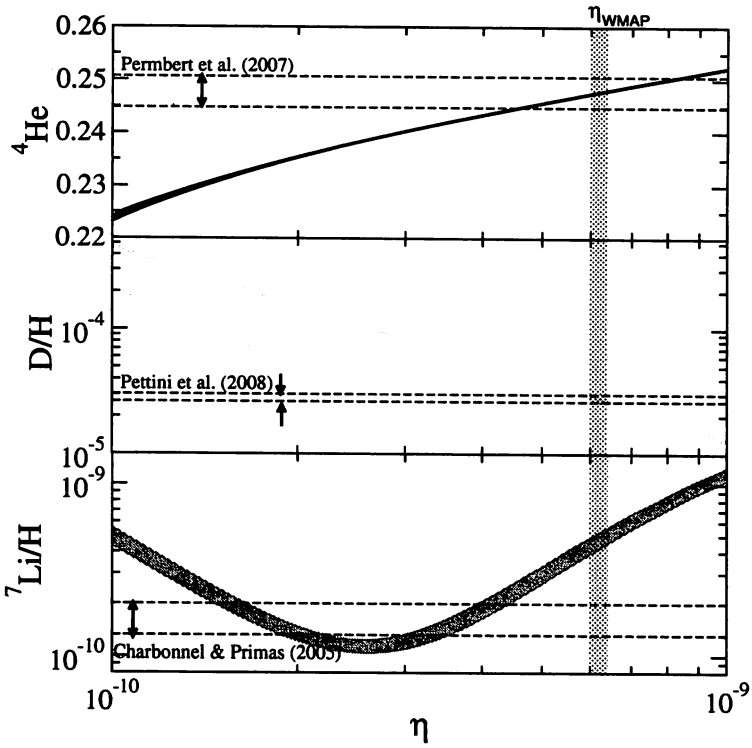

Fig. 2. Abundance of light elements produced in SBBN as a function of η. The vertical hatched region $\eta_{WMAP} = (6.19 \pm 0.15) \times 10^{-10}$ indicates the constraint from WMAP.[15]

the errors attached to the nuclear reaction rates of NACRE. Although a new decay rate of free neutrons $\tau_N = 878 \pm 0.7 \pm 0.3$ sec yields[28] $Y_p \simeq 0.245$, we adopt the conservative rate considering the uncertainty of the half life.[29]

As against the excellent agreement for D and ^{4}He, the discrepancy for ^{7}Li is unallowable. To solve this problem, we could rely on some unknown physical processes, nuclear reaction rates coupled with other reaction paths, and/or non standard models. It is noted that the observations of ^{7}Li involve uncertain atmospheric models concerning the low metallicity stars. The metallicity is measured usually from the abundance ratio relative to the solar value, e.g., [Fe/H]=log(Fe/H)$_{obs}$ - log(Fe/H)$_\odot$. Although the origin has been advocated to be cosmic spallation, puzzles of severe underproduction of ^{6}Li, ^{9}Be and ^{11}B in SBBN would be attributed to non standard scenario.

3.1. *Neutrino degeneracy*

Effects of neutrino degeneracy associated with β-decays have been investigated.[30] Our consideration is restricted to the inconsistency of the ^{7}Li abundance in low metallicity stars. The degeneracy would change the ratio ^{6}Li/^{7}Li which depends on the rate of D$(\alpha,\gamma)^6$Li reaction. Figure 3 shows the abundance of ^{6,7}Li and ^{11}B with including neutrino degeneracy[31] $\xi_i = \mu_i/kT$, where μ_i is the chemical potential of neutrinos. The uncertain ranges due to the cross sections of NACRE[24] are

illustrated by the bands. Also shown is the observational constraint by the vertical lines.[32),33)] Two upper limits deduced from low metallicity stars [Fe/H] $\simeq -3$ are $^6\mathrm{Li}/^7\mathrm{Li} \leq 0.052 \pm 0.0019$ and $\mathrm{B/H} \leq (3-6) \times 10^{-12}$. The produced abundances of ^{6}Li and ^{11}B could be highly affected by neutrino degeneracy through η, since they shift significantly to higher densities due to rapid expansion. Precise determination of the cross sections of $\mathrm{D}(\alpha,\gamma)^6\mathrm{Li}$ and $^7\mathrm{Li}(\alpha,\gamma)^{11}\mathrm{B}$ should give an insight into not only primordial abundances of Li-Be-B but the dark baryon density.

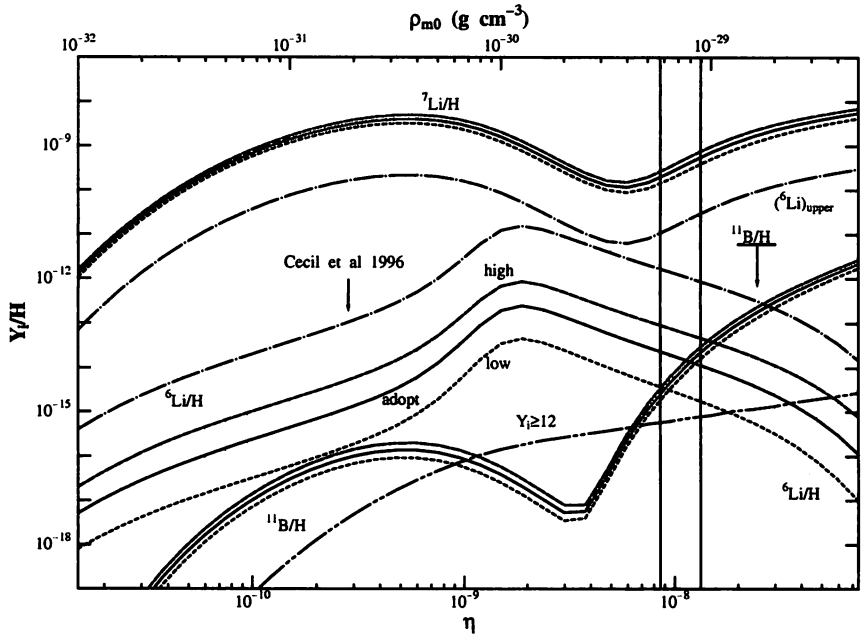

Fig. 3. Abundances of ^{6,7}Li and ^{11}B produced in a neutrino degenerate model with $\xi_e = 1.29$ and $\xi_\mu = 20$.

§4. Inhomogeneous big bang nucleosynthesis

A new astrophysical site of BBN is presented[22)] that contains very high η. In Fig. 4 we show the evolution of abundance for $\eta = 10^{-4}$, where neutrons are still left when heavy elements are synthesized. Stable nuclei with the mass number $A = 90$ are first synthesized with being followed by proton rich nuclei. On the other hand, other stable nuclei with $A = 158$ are synthesized through neutron rich nuclei. Figure 5 shows the similar results for $\eta = 10^{-3}$, where almost all neutrons are consumed before heavy elements are produced appreciably. The number fractions relative to the solar system abundances are shown in Fig. 6 for $\eta = 10^{-5} - 10^{-2}$. Note that the mass number of the produced elements is the largest at $\eta \simeq 10^{-4}$. The problem to be solved is the origin and evolution of the high density region. The size of the high density island is estimated[22)] to be $10^5 - 10^{17}$ cm at the BBN epoch. The upper bound is obtained from the maximum angular resolution of CMB and the lower is

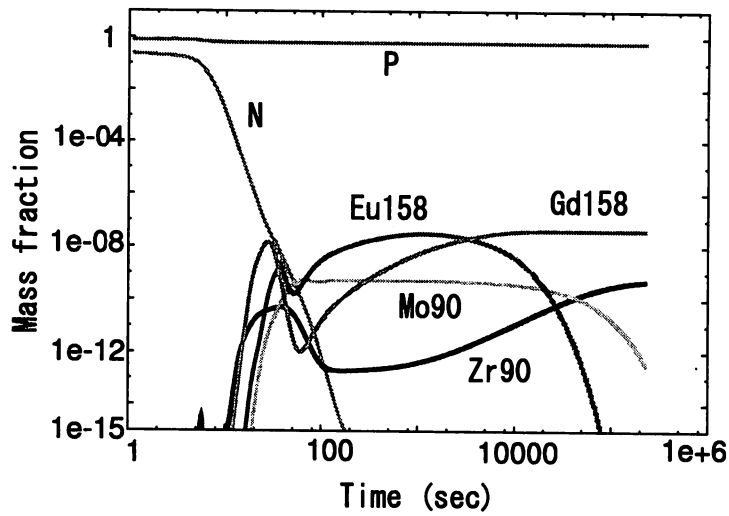

Fig. 4. Evolution of mass fractions in a high density region[22] with $\eta = 10^{-4}$.

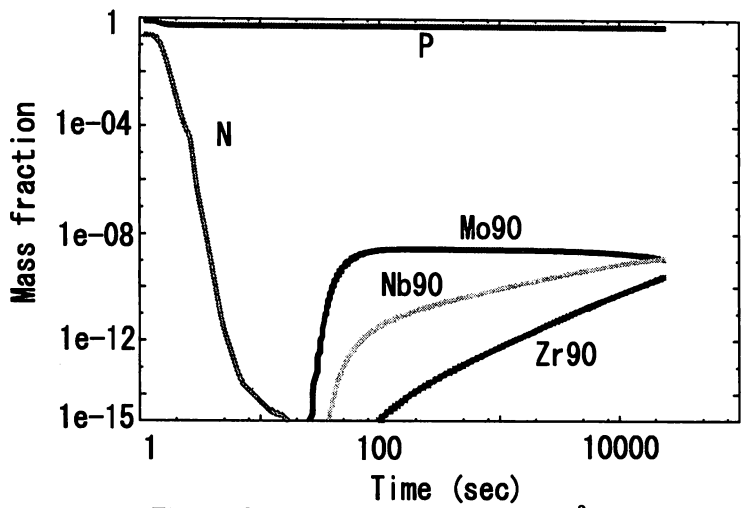

Fig. 5. Same as Fig. 4 but for $\eta = 10^{-3}$.

from the analysis[7] of comoving diffusion length of neutrons and protons.

Some models of baryogenesis suggest that very high baryon density regions form in the early universe. Recent observations, however, suggest that heavy elements could already exist in high red-shift epochs and therefore the origin of these elements becomes a serious problem. Motivated by these facts, we investigate BBN in very high baryon density regions. BBN proceeds in proton rich environment, which is regarded as a rapid p-process. However, by taking heavy nuclei into account, we find that BBN proceeds through both p- and r-processes simultaneously. Furthermore, p-nuclei such as ^{92}Mo, ^{94}Mo, ^{96}Ru and ^{98}Ru, whose origin is not well known, are

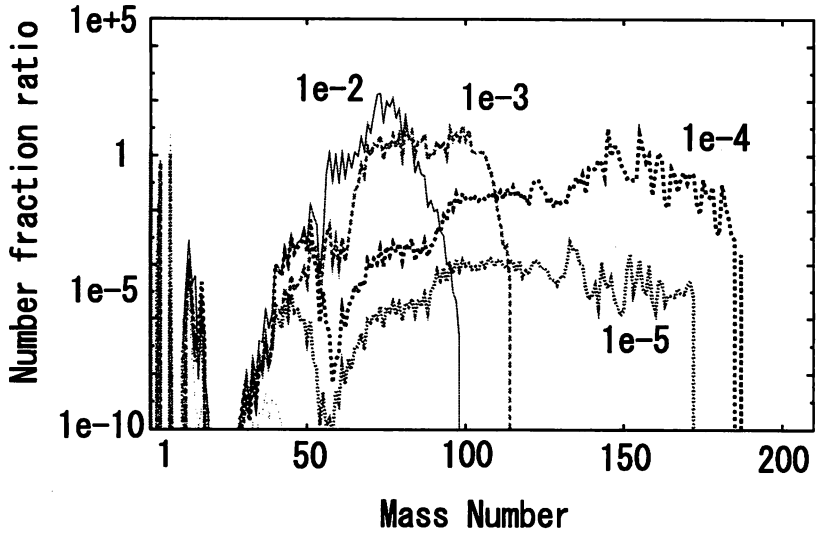

Fig. 6. Number fractions relative to the solar system abundances.[22]

also synthesized. The above issues should be refined and checked by investigating the possible model consistent with available observations.

4.1. *Two-zone model of IBBN*

Quite interesting features[22] have been presented for the possibility of IBBN, but relevant parameters concerning the high and low density regions have not yet been specified. Therefore, we explore the reasonable parameters using a simple two-zone model.[8] The early universe is assumed to contain high and low baryon density regions. For simplicity we ignore the diffusion effects.

We assume that all the produced elements are mixed homogeneously at some epoch between the end of BBN and the recombination era. To construct a two-zone model, we need to define n_{ave}, n_{high} and n_{low} as the average-, high-, and low-number densities of baryons, f_v as the volume fraction of the high baryon density region, and X_i^{ave}, X_i^{high} and X_i^{low} as the mass fractions of element i in the average-, high- and low-density regions, respectively. Then the basic relations between these variables are written as

$$n_{ave} = f_v n_{high} + (1 - f_v)\, n_{low}, \tag{4.1}$$

$$n_{ave} X_i^{ave} = f_v n_{high} X_i^{high} + (1 - f_v)\, n_{low} X_i^{low}. \tag{4.2}$$

If the baryon fluctuation is assumed to be isothermal,[6),11),12)] then Eqs. (4.1) and (4.2) are divided by the number density of photons n_γ to be

$$\eta_{ave} = f_v \eta_{high} + (1 - f_v)\eta_{low}, \tag{4.3}$$

$$\eta_{ave} X_i^{ave} = f_v X_i^{high} \eta_{high} + (1 - f_v) X_i^{low} \eta_{low}. \tag{4.4}$$

Here η's are

$$\eta_{ave} = \frac{n_{ave}}{n_\gamma}, \qquad \eta_{high} = \frac{n_{high}}{n_\gamma}, \qquad \eta_{low} = \frac{n_{low}}{n_\gamma},$$

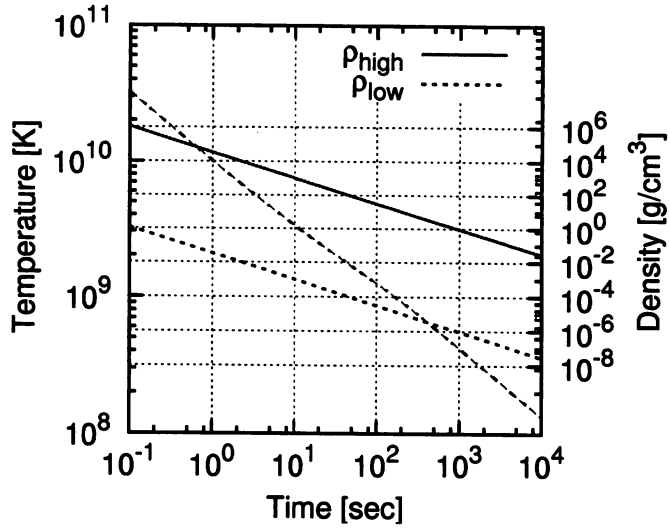

Fig. 7. Temperature and baryon densities for $f_\nu = 10^{-4}$ and $R = 10^6$.

where η_{ave} is set to be the observed value[15] $\eta_{\rm WMAP} = 6.1 \times 10^{-10}$. Both η_{high} and η_{low} are determined from f_ν and the density ratio $R = n_{high}/n_{low} = \eta_{high}/\eta_{low}$.

We note that ρ_b is the average baryon density obtained from Eq. (4.1), and temperature T is set to be homogeneous. This assumption is critically important to build our model; otherwise we must treat the zones to evolve separately, which involves fundamental problem as opposed to the cosmological principle.

Figure 7 shows the temperature (dashed line) and the baryon densities against time in the IBBN model with $f_\nu = 10^{-4}$ and $R = 10^6$. Note that ρ_{low} is nearly equal to that in SBBN, while ρ_{high} becomes very large. This indicates that nucleosynthesis in individual regions yields quite different elements.

4.2. *Constraints from light-element abundances*

We show in Fig. 8 an example of light element synthesis in the high and low density regions with $f_\nu = 10^{-6}$ and $R = 10^6$ that correspond to $\eta_{high} = 3.05 \times 10^{-4}$ and $\eta_{low} = 3.05 \times 10^{-10}$. In the right panel with η_{low} the evolution of the elements is almost the same as that of SBBN. In the left panel with η_{high}, D and ^{4}He are synthesized at higher temperatures. This is because the reaction $p + n \to {\rm D} + \gamma$ starts at earlier epoch. In addition the amount of ^{4}He is larger than that in the low density region, because neutrons still remain when nucleosynthesis starts. On the other hand, ^{7}Li (or ^{7}Be) is much less produced. It implies that heavier nuclei, such as ^{12}C and ^{16}O, are synthesized in the high density region. Using these calculated abundances in both regions, we obtain the average values of the light elements from Eq. (4.4). Then we can put constraints on f_ν and R by comparing the values of $Y_{\rm p}$ and D/H with the observed abundances.

The constraints are shown in Fig. 9 on the $f_\nu - R$ plane with the contours of η_{high}. In our analysis, we obtain only the upper limit to the parameter R. Note that the allowed region includes as very high density region as $\eta_{high} = 10^{-3}$.

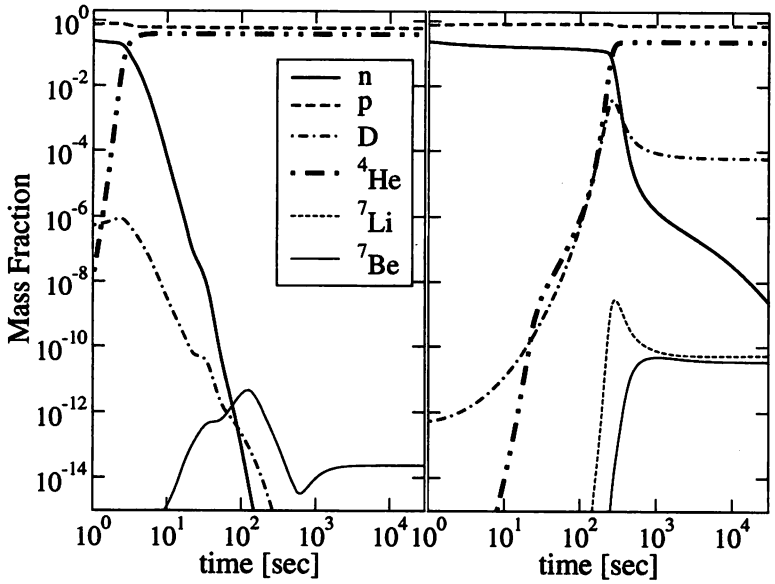

Fig. 8. Evolution of light elements in IBBN with $f_v = 10^{-6}$ and $R = 10^6$. The left panel indicates the high density region $\eta_{high} = 3.05 \times 10^{-4}$. The right panel is the low density region $\eta_{low} = 3.05 \times 10^{-10}$.

Since η_{high} takes a larger value, nuclei heavier than ^{7}Li are synthesized more and more. Then we estimate the abundance of CNO elements in the allowed region. Figure 10 shows the contours of the summation of X_i^{ave} over heavier nuclei ($A > 7$). As far as our small BBN code is concerned, the total mass fraction of CNO nuclei amounts to $X(A > 7) \simeq 10^{-7}$.

4.3. *Synthesis of heavy elements in high density region*

We investigate synthesis of heavy elements in the high-density region considering the constraints shown in Fig. 9. The evolution of temperature and density is the same as in the previous subsection. The abundance change is calculated with a large nuclear reaction network, which contains 4463 nuclei from neutron, proton to Americium ($Z = 95$ and $A = 292$). The nuclear data such as reaction rates, nuclear masses and partition functions are the same as used in Ref. 34) except for the weak interaction rates[35] which is adequate for the high temperature stage $T > 10^{10}$ K. Note that the mass fractions of ^{4}He and D obtained with the large network are consistent with those calculated with a small network in §4.2 within an accuracy of a few percents.

As seen in Fig. 10, heavy elements are produced at the level $X(A > 7) \geq 10^{-9}$ nearly along the upper limit of R in the allowed region. To examine the efficiency of the heavy element production, we select five models with parameters $\eta_{high} = (1, 5.5, 10.2, 53, 106) \times 10^{-5}$, which are indicated by the filled squares in Fig. 9.

Table I gives the abundance of light elements in the high and low density regions for Case A with $\eta_{high} = 1.02 \times 10^{-4}$ and Case B with $\eta_{high} = 1.06 \times 10^{-3}$. The mass fractions in the low density region (the second columns) are same as those obtained

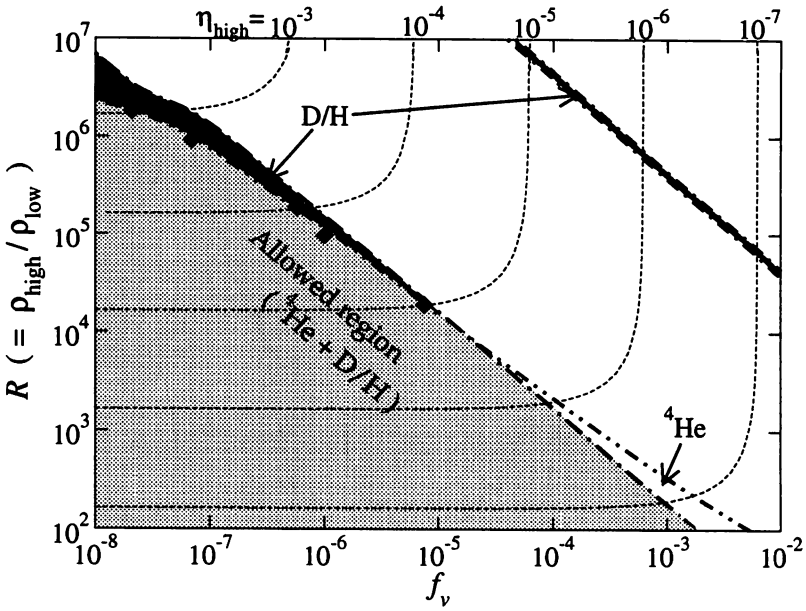

Fig. 9. Constraints on the $f_\nu - R$ plane from the observed abundance of light elements. The double dots-dashed line is derived from Y_p and the dot-dashed line is from D/H. The shaded region is allowed from both Y_p and D/H. The dotted lines indicate the contours of η_{high}. The filled squares indicate the parameters for which synthesis of heavy elements is examined in §4.3.

in § 3, because the abundance flows beyond $A = 7$ are negligible. We should note that the averages of Y_p and D/H coincide with the observed abundances (3.1) and (3.2).

In the high density region of Case A, the nucleosynthesis paths proceed along the stable line during a few seconds, and afterwards they are classified with the mass number. For nuclei with $A \leq 100$, proton captures become very active compared to neutron capture at $T > 2 \times 10^9$ K and the path shifts to the proton rich side, which begins from breaking out the hot CNO cycle. For nuclei of $100 < A < 120$, the path goes across the stable nuclei from proton- to neutron-rich side, since temperature decreases and the number of seed nuclei of neutron capture increases significantly. Neutron captures become much more efficient for heavier nuclei of $A \geq 120$. The neutron capture is not similar to the canonical $r-$process, since the nuclear reactions proceed under the condition of the high-abundance of protons. For example, ^{159}Tb, ^{159}Gd and ^{159}Eu are synthesized through neutron captures. After $t = 10^3$ sec, we can see β-decays $^{159}\text{Eu} \rightarrow {}^{159}\text{Gd} \rightarrow {}^{159}\text{Tb}$, where the lifetimes of ^{159}Eu and ^{159}Gd are 10.1 min and 18.479 h, respectively.

In Case B the reactions also first proceed along the stable line in the high density region. Subsequently, the reactions directly proceed to the proton-rich side through rapid proton captures. We can see β-decays $^{108}\text{Sn} \rightarrow {}^{108}\text{In} \rightarrow {}^{108}\text{Cd}$, where the lifetimes of ^{108}Sn and ^{108}In are 10.3 min and 58.0 min, respectively. In addition, radioactive nuclei ^{56}Ni and ^{57}Co are produced just after the formation of ^{4}He in the extremely high density region with $\eta_{high} \geq 10^{-3}$ like the beginning of supernova

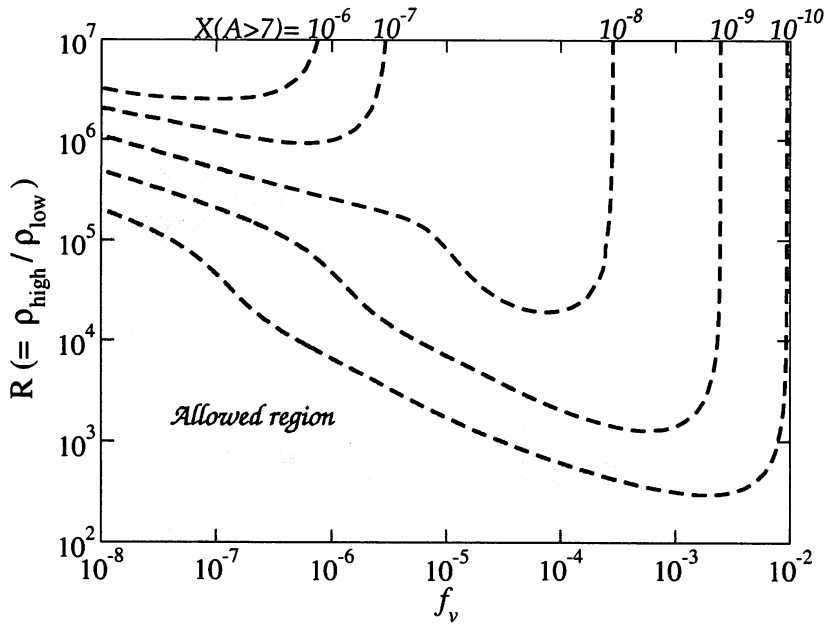

Fig. 10. Contours of the total mass fractions of heavier nuclei ($A > 7$). The shaded allowed region is the same as in Fig. 9.

explosions.[36]

Figure 11 shows the evolutions of the neutron abundances for relevant values of η_{high}. When $\eta_{high} = 10^{-3}$, the neutron abundance decreases immediately at $t \simeq 10$ sec because of the rapid production of ^{4}He and ^{56}Ni. Therefore, the neutron abundance is not enough for neutron capture to produce heavy nuclei of $A > 90$. On the contrary, neutrons still remain even at high temperatures for the lower value of η_{high}. If $\eta_{high} = 10^{-4}$, neutrons are left to induce the neutron captures. Note that, as seen from Fig. 6, synthesis of heavy elements beyond $A \simeq 50$ becomes inefficient for $\eta < 10^{-4}$.

The decrease in time scales change drastically the flow of BBN. When $\eta_{high} = 5.3 \times 10^{-4}$, nucleosynthesis proceeds along the stable line by way of the neutron induced reactions before the significant decrease in the neutron abundances at $t \simeq 10$ sec. At that time, the nuclear reactions are stuck around $Z = 60$ with $N = 82$, since it takes long time to synthesize heavier nuclei because there are stable isotopes Nd ($Z = 60$) and Sm ($Z = 62$). As time goes, neutron captures start by these nuclei and r-elements can be synthesized. After the depletion of neutrons at $t \simeq 40$ sec, nuclei around the neutron numbers $N = 82$ like ^{144}Sm are produced through proton induced reactions.

In Case A a lot of nuclei of $A > 7$ are synthesized whose amount is comparable to that of ^{7}Li. The yields include both s-element ^{138}Ba and r-elements such as ^{142}Ce and ^{148}Nd, since moderate amounts of neutrons remain as shown in Fig. 11.

In Case B there are few r-elements, though both s-elements ^{82}Kr and ^{89}Y and p-elements ^{74}Se and ^{78}Kr are synthesized. A significant amount of heavy elements

Table I. Mass fractions of light elements in IBBN. t_{fin} and T_{fin} are the time and temperature at the final stage of our calculations.

Case A

f_v, R	1.0×10^{-7},	1.7×10^{5}	
η_{high}, η_{low}	1.02×10^{-4},	6.00×10^{-10}	
t_{fin}, T_{fin}	1.2×10^{5} sec,	4.3×10^{7} K	
elements	high	low	average
p	0.638	0.752	0.750
D	6.84×10^{-22}	4.34×10^{-5}	4.27×10^{-5}
^{3}He	2.9×10^{-14}	2.2×10^{-5}	9.3×10^{-6}
^{4}He	0.362	0.248	0.249
^{7}Li	7.42×10^{-13}	1.87×10^{-9}	1.70×10^{-9}

Case B

f_v, R	2.1×10^{-8},	1.8×10^{6}	
η_{high}, η_{low}	1.06×10^{-3},	5.88×10^{-10}	
t_{fin}, T_{fin}	1.0×10^{5} sec,	4.2×10^{7} K	
elements	high	low	average
p	0.586	0.753	0.746
D	1.76×10^{-21}	4.48×10^{-5}	4.32×10^{-5}
^{3}He	2.9×10^{-14}	2.2×10^{-5}	9.3×10^{-6}
^{4}He	0.413	0.247	0.253
^{7}Li	1.63×10^{-13}	1.79×10^{-9}	1.72×10^{-9}

$A \leq 90$ is produced owing to the explosive nucleosynthesis under the high density circumstances ($\rho \simeq 10^6$ g cm^{-3}). The most abundant element is found to be ^{56}Ni. The produced amount is much larger than the upper limit of the mass fraction derived from the usual calculations with the BBN code, because our BBN code used in § 3 contains the elements up to ^{16}O and the actual abundance flow proceeds to much heavier elements.

Figure 12 shows the averaged abundances X_i^{ave} compared with the solar system abundances.:[37] When $\eta_{high} \simeq 10^{-4}$, the produced abundance of $120 < A < 180$ is comparable to the solar values, while nuclei of $50 < A < 100$ have been synthesized well for $\eta_{high} \simeq 10^{-3}$. If $\eta_{high} = 5.3 \times 10^{-4}$, there are outstanding two peaks around $A = 56$ ($N = 28$) and around $A = 140$. The abundance pattern is very different from that of the solar system, because IBBN occurs under the peculiar condition of abundant neutrons and protons.

Finally we show in Fig. 13 the evolution of abundances which are classified in the solar system abundances as pure nuclei of s, r and p-elements. We remark the coexistence of Xe isotopes produced simultaneously. These isotopic anomalies[38] observed in many samples of meteorites are regarded as a long-standing problem. Our IBBN model, therefore, could present a clue to solve this problem.

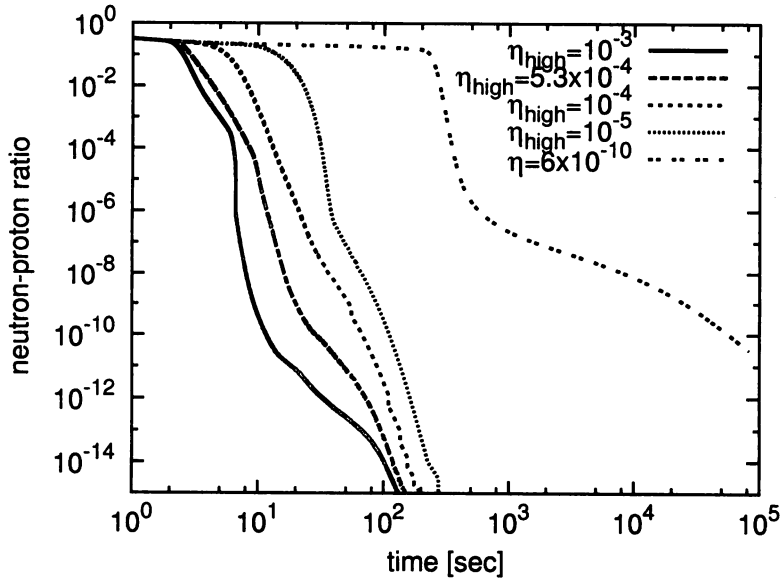

Fig. 11. Evolution of the neutron abundances. The double dots line indicates SBBN with $\eta = 6.1 \times 10^{-10}$. The others indicate the high density regions in IBBN.

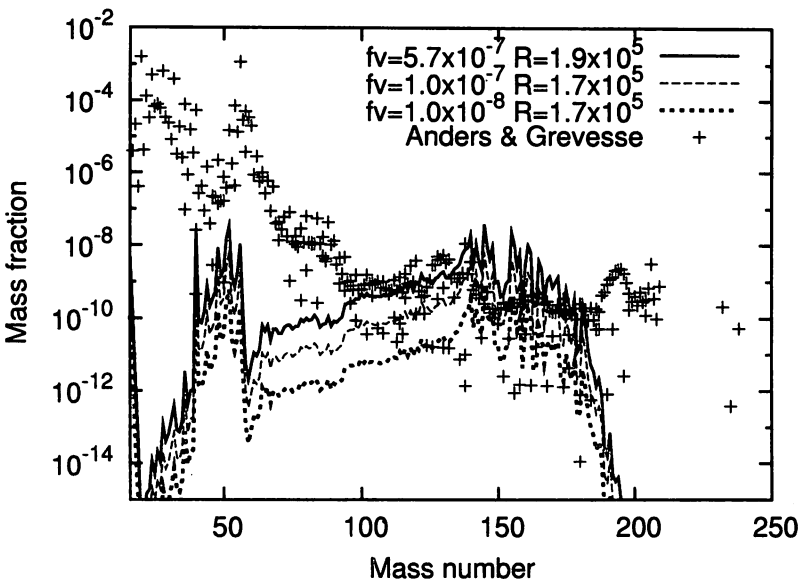

Fig. 12. Comparison of the averaged mass fractions for $\eta_{high} = 10^{-4}$.

§5. Summary and discussions

We have compared the results of SBBN with the current observations of light elements. Considering the uncertainties in the nuclear reaction rates and the observed errors, we can summarize as follows:

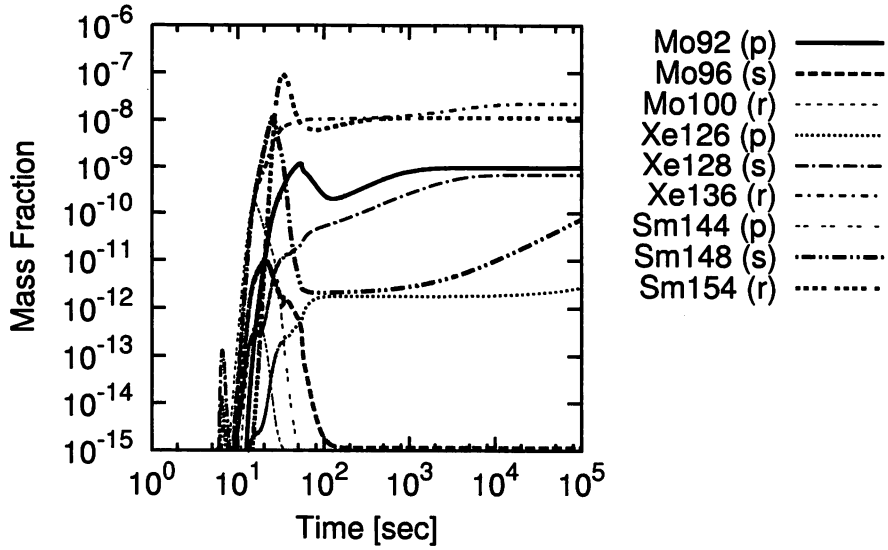

Fig. 13. Evolutions of the averaged mass fraction of pure nuclei for $\eta_{high} = 10^{-4}$.

(1) The consistency is confirmed as far as ^{4}He and D are concerned.

(2) Large uncertainties of He observations may indicate some unknown processes beyond SBBN. For example, a large value of $Y_p \simeq 0.3$ has been reported in low metallicity stars in globular clusters.[39]

(3) The significant discrepancy in ^{7}Li remains to be solved.

(4) Underproduction of ^{6,7}Li and/or ^{11}B might be ascribed to some uncertain nuclear reaction rates coupled to non-standard model loaded with neutrino degeneracy.

The consistency between IBBN and the observations of ^{4}He and D/H abundances has been investigated under the thermal evolution of the standard model with $\eta_{\rm WMAP}$. We have examined the two-zone model, where the universe has the high and low baryon density regions separately at the BBN epoch. We have calculated nucleosynthesis that covers 4463 nuclei in the high density region. Below we summarize our results and give some prospects.

(1) There are significant differences for the evolution of the light elements between the high and low density regions; In the high density region, nucleosynthesis begins at higher temperature. ^{4}He is more abundant than that in the low density region. Using the observed abundances of ^{4}He and D/H, we have constrained two parameters in IBBN: the volume fraction f_v and the density ratio R.

(2) Both p- and r-elements are synthesized simultaneously in the high density region with $\eta_{high} \simeq 10^{-4}$. Total mass fractions of heavier elements than ^{7}Li amount to 10^{-7} for $\eta_{high} = 10^{-4}$ and 10^{-5} for $\eta_{high} = 10^{-3}$. The average mass fractions in IBBN are comparable to the solar system abundances. There exist over-produced elements around $A = 150$ (for $\eta_{high} = 10^{-4}$) and $A = 80$ (for $\eta_{high} = 10^{-3}$). We

suspect the results to be in conflict with the chemical evolution in the universe. It is, however, possible to find permissible parameters to avoid the overproduction.

(3) Heavy elements beyond Fe surely affects the formation process of the first generation stars due to the change in the opacity. Therefore, it may be also necessary for IBBN to be constrained from the star formation scenarios.

(4) Although underestimation of observed abundance[40] of ^{7}Li cannot be explained in terms of SBBN, our IBBN model may conduce to the answer. A reasonable abundance of ^{7}Li can be synthesized not only in the low density region but high density one with adjusting η.

(5) Although we have ignored the diffusion effects so far, it is shown that they affects IBBN significantly.[8] Evolution and distribution of high density regions in the sea of low density plasma should be explored considering a statistical analysis.

(6) Because IBBN could provide a clue to solve the long-standing problem of isotopic anomalies in meteorites, comparison between the produced amounts and the observed abundance leads to constrain to our IBBN model.

Acknowledgements

This work has been supported in part by a Grant-in-Aid for Scientific Research (19104006, 21540272) of the Ministry of Education, Culture, Sports, Science and Technology of Japan.

References

1) R. A. Alpher, H. Bethe and G. Gamow, Phys. Rev. **73** (1948), 803.
C. Hayashi, Prog. Theor. Phys. **5** (1950), 224.
R. V. Wagoner, W. A. Fowler and F. Hoyle, Astrophys. J. **148** (1967), 3.
G. Steigman, Ann. Rev. Nucl. Part. Sci. **57** (2007), 463.
F. Iocco et al., Phys. Rept. **472** (2009), 1.
2) V. Luridiana et al., Astrophys. J. **592** (2003), 846.
Y. I. Izotov, T. X. Thuan and G. Stasinska, Astrophys. J. **662** (2007), 15.
D. Kirkman et al., Astrophys. J. Suppl. **149** (2003), 1.
M. Pettini et al., Mon. Not. Roy. Astron. Soc. **391** (2008), 1499.
J. M. O'Meara et al., Astrophys. J. **649** (2006), L61.
3) M. Permbert et al., Astrophys. J., **666**, (2007), 636.
4) S. G. Ryan et al., Astrophys. J. **530** (2000), L57.
P. Bonifacio, et al., Astron. Astrophys. , **462** (2007), 851.
5) A. Coc et al., Astrophys. J. **600** (2004), 544
R. H. Cyburt, B. D. Fields and K. A. Olive, JCAP **0811** (2008), 012.
6) N. Terasawa and K. Sato, Phys. Rev. D **39** (1989), 2893.
K. Jedamzik, and J. B. Rehm, Phys. Rev. D **64** (2001), 023510.
T. Rauscher et al., Astrophys. J. **429** (1994), 499.
7) J. H. Applegate, C. J. Hogan and R. J. Scherrer, Phys. Rev. D **35** (1987), 1151.
8) R. M. Malaney and W. A. Fowler, Astrophys. J. **333** (1988), 14.
J. H. Applegate, C. J. Hogan, R. J. Scherrer, Astrophys. J. **329** (1988), 572.
N. Terasawa and K. Sato, Astrophys. J. **362** (1990), L47.
D. Thomas et al., Astrophys. J. **430** (1994), 291.
9) K. Jedamzik, G. M. Fuller, G. J. Mathews and T. Kajino, Astrophys. J. **422** (1994), 423.
10) S. Matsuura, A. D. Dolgov, S. Nagataki and K. Sato, Prog. Theor. Phys. **112** (2004), 971.
11) C. Alcock, G. M. Fuller and G. J. Mathews, Astrophys. J. **320** (1987), 439.
12) G. M. Fuller, G. J. Mathews and C. R. Alcock, Phys. Rev. D **37** (1988), 1380.
H. Kurki-Suonio and R. A. Matzner, Phys.Rev. D **39** (1989), 1046; *ibid.* D **42** (1990),

1047.
13) Y. Aoki et al., Nature **443** (2006), 675.
14) C.L. Bennett, et al., Astrophys. J. Suppl. **148** (2003), 1.
D. N. Spergel et al., Astrophys. J. Suppl. **170** (2007), 377.
J. Dunkley et al., Astrophys. J. Suppl. **180** (2009), 306.
15) E. Komatsu et al., astro-ph. CO 1001.4538 (2010).
16) M. Hashimoto and K. Arai, Phys. Rep. Kumamoto Univ. **7** (1985), 47.
17) Y. Juarez et al., Astron. Astrophys. **494** (2009), L25.
18) T. Moriya and T. Shigeyama, Phys. Rev. D **81** (2010), 043004.
19) L. R. Bedin et al., Astrophys. J. **605** (2004), L125.
G. Piotto et al., Astrophys. J. **661** (2007), L53.
20) T. Rauscher, Phys. Rev. D **75** (2007), 068301.
21) S. Matsuura, S. I. Fujimoto, S. Nishimura, M. A. Hashimoto and K. Sato, Phys. Rev. D **72** (2005), 123505.
22) S. Matsuura, S. I. Fujimoto, M. A. Hashimoto and K. Sato, Phys. Rev. D **75** (2007), 068302.
23) R. Nakamura, M .Hashimoto, S. Gamow and K. Arai, Astron. Astrophys. **448** (2006), 23.
24) C. Angulo et al., Nucl. Phys. A **656** (1999), 3.
25) K. Hagiwara et al., Phys. Rev. D **66** (2002), 010001.
26) M. Pettini et al., Mon. Not. Roy. Astron. Soc. **391** (2008), 1499.
27) C. Charbonnel and F. Primas, Astron. Astrophys. **442** (2005), 961.
28) G. J. Mathews, T. Kajino and T. Shima, Phys. Rev. D, **71** (2005), 021302.
29) A. P. Serebrov et al., Phys. Lett. B **605**, (2005), 72.
A. P. Serebrov et al., Phys. Rev. C **78**, (2008), 035505.
30) K. Kohri, M. Kawasaki and K. Sato, Astrophys. J. **490** (1997) 72.
31) M. Hashimoto, M. Kamimura and K. Arai, Few–Body Systems Suppl. **12**, (2000), 92.
32) S. Burles, D. Kirkman and D. Tytler, Astrophys. J. **519**, 18, 1999.
33) K. Arai, M. Hashimoto and T. Wakita, Phys. Rept. Kumamoto Univ. **11** (2000), 37.
34) S. Fujimoto, M. Hashimoto, O. Koike, K. Arai and R. Matsuba, Astrophys. J. **585** (2003), 418.
O. Koike, M. Hashimoto, R. Kuromizu and S. Fujimoto, Astrophys. J. **603** (2004), 592.
S. Fujimoto, M. Hashimoto, K. Arai and R. Matsuba, Astrophys. J. **614** (2004) 847.
S. Nishimura, K. Kotake, M. Hashimoto, S. Yamada, N. Nishimura, S. Fujimoto and K. Sato, Astrophys. J. **642** (2006), 410
35) L. Kawano, FERMILAB-Pub-92/04-A
36) M. Hashimoto, Prog. Theor. Phys. **94** (1995), 663.
37) E. Anders and N. Grevesse, Geochim. Cosmochim. Acta **53** (1989), 197.
38) M. Rayet, M. Arnould, M. Hashimoto, N. Prantzos and K. Nomoto, Astron. Astrophys. **298** (1995), 517.
39) Y. Izotov and T. X. Thuan, Astrophys. J. **710** (2010), L67.
40) A. J. Korn et al., Nature **442** (2006), 657.